Available online at www.sciencedirect.com
SCIENCE DIRECT®
Journal of Molecular Catalysis A: Chemical 237 (2005) 67–79
JOURNAL OF MOLECULAR CATALYSIS A: CHEMICAL
www.elsevier.com/locate/molcata

Hydrogenation of edible oil over Pd catalysts: A combined theoretical and experimental study

María B. Fernández, Gabriela M. Tonetto, Guillermo H. Crapiste, María L. Ferreira *, Daniel E. Damiani

PLAPIQUI (UNS-CONICET), Camino La Carrindanga Km 7, CC 717, CP 8000 Bahía Blanca, Argentina

Received 25 February 2005; received in revised form 29 April 2005; accepted 30 April 2005
Available online 6 June 2005

Abstract

Studies on the hydrogenation of sunflower oil on supported Pd catalysts were performed. The reaction was investigated at 373 K and 413.5 kPa using a semi batch reactor.

The adsorption of oleic acid on Pd surface was modeled. The metal catalyst was represented by three low index planes while the oil by *cis*-4-decene. Besides, two different mechanisms were studied for the *cis*/*trans* isomerization and full hydrogenation of the oleic acid: Horiuti–Polanyi and adsorbed monoyne-mediated mechanism. The *cis*-4-decene model and all the subsequent reaction structures were conformationally studied by molecular mechanics (MM2). The more stable conformations were used as input for extended Hückel like calculations. The theoretical studies show that the selected mechanisms were energetically possible on the Pd planes, however the monoyne-mediated mechanism was more exothermic.

Keywords: Hydrogenation; Sunflower oil; *trans*-Isomers; Palladium; EHMO; MM2

1. Introduction

The hydrogenation process of vegetable oils is very important in the food industry. It is used to improve oxidative and thermal stability of the oil and to convert liquid oils to the semi-solid form.

The hydrogenation is usually carried out in a three-phase semi batch reactor: hydrogen gas is bubbled in hot liquid oil (393–461 K), usually under pressure (100–608 kPa), in the presence of a catalyst, typically powdered nickel. Simultaneously to double bonds saturation, partial hydrogenation of polyunsaturated oils causes isomerization of some of the remaining double bonds and migration of others, resulting in an increase in the *trans* fatty acid content and the hardening of fat.

The *trans* fatty acids have adverse health implications. Mensink and Katan [1] suggested that a diet enriched in elaidic acid, compared to one enriched in oleic acid, increased total and low-density lipoprotein (LDL) cholesterol concentrations and decreased high-density lipoprotein (HDL) cholesterol concentration, hence resulting in a less favorable total-cholesterol:HDL-cholesterol ratio. Ascherio et al. [2] demonstrated a dose-dependent relationship between *trans* fatty acid intake and the LDL:HDL ratio, and when combining a number of studies, the magnitude of this effect is greater for *trans* fatty acids compared to saturated fatty acids.

With this motivation, the demand for lower levels of *trans*-isomers content in hydrogenated edible oils has increased. A field in which there have been major advances is that of hydrogenation catalysts [3]. The bulky size of the triglyceride molecules, together with the simultaneity of other reactions, as those of positional or geometrical isomerization, can imply that the reaction is not insensible to the catalytic surface.

There are reports for the use of Pd catalysts in the hydrogenation of edible oils [4]. Because of the higher activity than its Ni predecessors, the operation can be carried out under softer conditions. The aim of the present study is to compare

* Corresponding author. Tel.: +54 291 4861700; fax: +54 291 4861600.
E-mail address: mlferreira@plapiqui.edu.ar (M.L. Ferreira).

1381-1169/$ – see front matter © 2005 Elsevier B.V. All rights reserved.
doi:10.1016/j.molcata.2005.04.047

Nomenclature

C	concentration (mol/m^3)
D	mean particle size (m)
D_{eff}	effective diffusion coefficient (m^2/s m$^3_{liq}$/m$^3_{cat}$)
E	energy
r_{obs}	observed rate (mol/s kg$_{cat}$)
TAG	triglyceride

Greek letters

Φ	Weisz–Prater criterion
ρ_p	catalyst apparent density (g/cm^3)

Sub- and superscripts

i	component
p	particle

the dependence of catalytic activity and *cis*/*trans* selectivity with the support features and metallic particle size, looking forward to lowering the *trans*-isomer content in the hydrogenated edible oils.

There are scarce reports in the open literature about the reactions of triglyceride model compounds on transition metals planes. On the other hand, there is a great number of reports of the modeling of the adsorption and/or reaction of 1-butene and 2-*cis*/*trans*-butenes on transition metals [5,6] mainly Pt, Pd and Ni. The reactions such as oxidative addition and reductive elimination were investigated from a theoretical point of view quite early, especially for H–H, C–H and C–C bonds with either naked metal atoms or with the $M(PH_3)_2$ fragment (M = Pd, Pt) [7–10]. The formation of the two M–H or M–C bonds requires the promotion of the metal to the d^9s^1 state. The more accessible this state is, the more exothermic the oxidative addition and the lowest the corresponding energy barrier are. This is why oxidative additions are generally easier with Pt than Pd systems. However, reductive elimination process is less difficult for Pd. There are no electrons in the Pd 5s orbital and this leads to a minimal repulsion with the incoming substrate and explains why the energy barriers are relatively moderate for CH_4, very low for C_2H_4, while no barrier exists for C_2H_2. The sideways orientation necessary for an efficient interaction between the metal and the C–H bond is easily reached by ethylene and acetylene. Stronger C–H bonds are also more easily activated, but the molecular precursors Pd-C_2H_4 or Pd-C_2H_2 have strong stability [11]. These molecular precursors act as thermodynamic sinks.

The interaction of 1,3-butadiene, 1-butene and 2-*cis*/*trans*-butenes with Pt(1 1 1) and Pd(1 1 1) surfaces has been studied by density functional theory (DFT) [12]. A same stable adsorption mode has been found on both metal surfaces with similar adsorption energies.

The triglycerides are bulky molecules. Sunflower oil exhibits a molar composition of oleic acid (18:1) and linoleic acid (18:2) of 35 and 52.6%, respectively. This paper reports experimental studies and theoretical calculation. We selected a model of oleic acid, *cis*-4 decene, to study the *cis*/*trans* isomerization and full hydrogenation over different Pd clusters using a molecular mechanics approach and molecular orbital calculations. We also presented experimental results of the hydrogenation of sunflower oil on supported Pd catalysts prepared using different precursors and supports. The reaction was investigated at 373 K and 413.5 kPa using a semi batch reactor.

2. Experimental

2.1. Catalysts preparation

Supported Pd catalysts were prepared following two different methods: wet impregnation (WI) and incipient-wetness impregnation (IWI). The support materials were γ-Al_2O_3 (Condea, Puralox, 137 m^2/g), α-Al_2O_3 (Rhone Poulenc, 9.5 m^2/g) and Na-ZSM5 (Chemie Uetikon AG, 346.7 m^2/g). Prior to impregnation the supports were dried under N_2 flow at 423 K for 2 h.

Na-ZSM5 was ion-exchanged to obtain the protonic acid form of the zeolite. Four ion exchanges were performed using 1 M NH_4NO_3 solution for 6 h at 353 K. The zeolite was washed and filtered three times between each ion exchange in order to secure that all the impurities were completely removed. Finally the catalyst pellets were calcined (4 h at 1393 K and 4 h at 833 K).

Pd(A)/γ-Al_2O_3 and Pd(A)/α-Al_2O_3 were prepared by WI of the support with a solution of $Pd(Acac)_2$ (Acac = $C_5H_7O_2$) in toluene, at 298 K for 24 h.

Pd(N)/γ-Al_2O_3 and Pd(N)/α-Al_2O_3 were prepared by impregnation of the support with solution of $Pd(NO_3)_2$ using the IWI method. The sample Pd(N)/ZSM5 was prepared by the same technique using $(NH_3)_4Pd(NO_3)_2$ as a precursor.

After impregnation the catalyst were dried in Ar at 423 K for 2 h and then heated in chromatographic air at 773 K for 2 h.

The palladium content was determined by atomic absorption spectroscopy.

2.2. H_2 chemisorption

Hydrogen chemisorption runs were carried out in a conventional pulse apparatus [13] at atmospheric pressure and 373 K. Prior to chemisorption the catalysts were reduced "in situ" at 573 K in flowing H_2. The fraction of exposed Pd was calculated assuming that one hydrogen atom is adsorbed per surface Pd metal atom.

2.3. Catalytic activity measurements

Hydrogenation tests were carried out in a 600 ml Parr reactor of operated in a semi-continue manner. The reactor

was connected to a hydrogen (AGA chromatographic grade) source, maintained at constant pressure. The H_2 consumption was measured during the reaction.

The catalytic tests were performed at 373 K and 413.5 kPa during 1 h and using 250 ml of refined sunflower oil. The catalyst weight was adjusted in order to keep constant the weight of exposed Pd among the various experiments and the stirring rate was 1400 rpm.

The reduced catalyst was added to the reactor (containing the sunflower oil at the reaction temperature). Then, the pressure was increased in order to start the reaction. The H_2 flow rate versus time curve was corrected for the identical experimental conditions without the catalyst was.

An AGILENT 4890D gas chromatograph (GC) equipped with a flame ionization detector (FID) was used to study the reaction products, following the procedures established by the AOCS Ce 1c-89 norm. A 60 m long SUPELCO 2380 capillary column, with a nominal diameter of 0.25 mm and a nominal film thickness of 0.20 μm was used for the separation of the different compounds present in the samples. The iodine number (IV) was calculated from the fatty acid composition following the AOCS Cd 1c-85 norm.

Since hydrogenation of edible oils is a three-phase process, several transport limitations may occur. The volumetric gas–liquid mass-transfer coefficient, $K_L a$, was separately measured at an excess of catalyst load [14]. Intra-particle diffusion limitations for hydrogen were estimated from the Weisz–Prater number [15].

3. Theoretical model

3.1. Extended Hückel molecular orbital

The Extended Hückel molecular orbital (EHMO) method developed by Hoffmann and co-workers [16–18] to study electronic structure of transition metal complexes and used to study adsorbed molecules. This provides useful qualitative trends in large system models. The electronic structure and molecular properties are determined from electron equations for the molecular orbitals. In this formalism, the non-diagonal elements of Hamiltonian of the system are considered proportional to the overlap matrix elements. More recently, Chamber et al. [19] and Anderson and Hoffman [20] introduced some corrections in order to improve the traditional Extended Hückel Hamiltonian including repulsive terms to the total energy.

The total energy of an adsorbed molecule is:

$$E_t = \sum_i n_i E_i + \frac{1}{2} \sum_i \sum_{i \neq j} E_{rep(i,j)} \quad (1)$$

The E_i energy term is related to the electrons in the valence level i with an occupancy n_i. The core–core repulsion energy is originated between all the possible pairs nucleus i-fixed atom j.

Atomic parameters are necessary for calculations, being the EHMO a semi-empirical method. We used reported ionization potential obtained from spectroscopic data [21]. Since for the level 4p only theoretical data are available in literature, we used the data from Hartree–Fock–Slater [22]. Parameters used in this work are presented in Table 1.

The program used to calculate the energy of the different adsorbed species was the ICONC, originally developed by Chamber et al. [19], which takes into account repulsive terms that are not originally considered in the EHMO.

The total energy of adsorbed species was calculated as the difference between the electronic energy of the system when the adsorbed molecule is at a finite distance from the surface and when the molecule is far away from the cluster surface. The geometry optimization was done at 0.1 Å steps and, due to the approximate nature of extended Hückel like methods, the convergence criterion to the energy was set to 0.01 eV.

The semi-empirical molecular orbital calculations have been performed in the framework of the cluster approximation, that is the adsorption site and its neighborhood were modeled by a portion of the otherwise infinite solid.

The adsorption energy was calculated by: subtracting to the total energy of the adsorption system the energy corresponding to the free molecule and to the metallic cluster:

$$\Delta E_{ads} = \Delta E_{molecule/cluster} - \Delta E_{molecule} - \Delta E_{cluster}$$

where $E_{molecule/cluster}$ is the adiabatic energy when the molecule/specie is on the surface, $E_{molecule}$ is the energy for the molecule/specie in vacuum and the $E_{cluster}$ is the energy for a clean surface.

3.2. Molecular mechanics version 2-MM2

The Chem 3D 5.0 (from Cambridge Soft) was used. It contains a modified version of Allinger MM2 force field.

Table 1
Atomic parameters used for EHMO calculation

Atom	Orbital	Ionization potential (eV)	Slater exponent	Linear coefficient
Pd	5s	−7.24	2.19 (ξ_1)	
	5p	−3.68	2.15 (ξ_1)	
	4d	−11.90	5.98 (ξ_1), 2.61 (ξ_2)	0.55 (c_1), 0.67 (c_2)
H	1s	−13.60	1.00 (ξ_1)	
C	2s	−15.59	1.5536 (ξ_1)	
	2p	−10.26	1.4508 (ξ_1)	

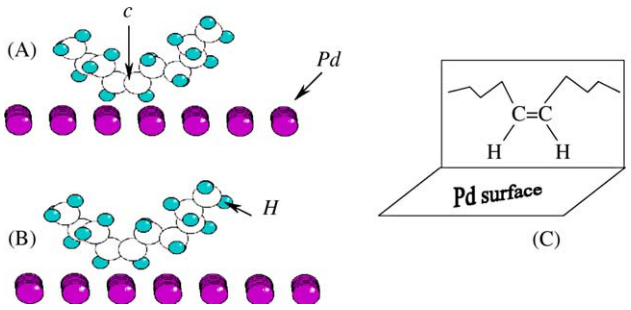

Fig. 1. *cis*-4-Decene over Pd(1 1 0): (A) di-σ adsorption; (B) π adsorption; (C) schematic molecule-surface relationship.

The principal additions are a charge-dipole interaction term, a quartic stretching term, cutoffs for electrostatic and van der Waals terms with fifth order polynomial switching function, automatic "pi" system calculations when necessary and torsional and non-bonded constraints. The parameter table of Chem 3D contains many adjustable parameters that correct for the failing of many of the potential functions in outlying situations.

MM2 was used to conformationally study the *cis*-4-decene model and all the subsequent reaction structures. The more stable conformations were used as input for EHMO calculation.

3.3. Modeling of surface palladium structures

Pd has a fcc structure with a lattice of 3.891 Å. This value leads to a triangular array (hexagonal close-packed) with a Pd–Pd distance of 2.70 Å. Three planes were modeled:

- Pd(0 0 1): A cluster of 63 atoms was used to represent this face. The Pd atoms were arranged in two layers of 32 (first layer) and 31 (second layer)atoms.
- Pd(1 1 1): A Pd cluster containing 85 atoms, distributed in two layers of 46 (first layer) and 39 (second layer) atoms.
- Pd(1 1 0): A cluster of 83 Pd atoms, distributed in two layers of 48 (first layer) and 35 (second layer) atoms.

The dangling bonds were sutured by hydrogen atoms. The palladium atoms were distributed in two layers as it is shown in Fig. 1. No surface relaxations were considered [23].

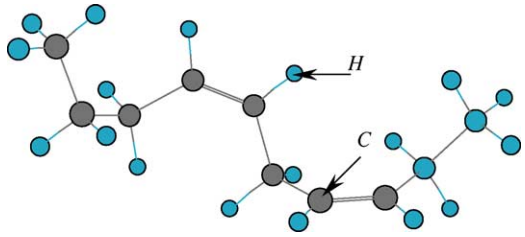

Fig. 2. L#1 model side view.

The EHMO allowed us to simulate a cluster of considerable number of sites, which is more computing demanding. Our aim was to simulate the effects of bulky molecules such as those of vegetable oils hydrogenation and their interaction with the metallic surfaces, including the steric interactions.

3.4. Model compounds

cis-4-Decene was used to represent oleic acid (Fig. 1). The double bond can adsorb in a di-σ or π configuration. In the former case, two C atoms in the double bond are adsorbed forming a σ union with the metal. The second case involves the formation of a π-allylic radical, in which the three C atoms are implicated with the active site.

The *cis*-4,*cis*-7-decediene molecule was selected as a model compound for linoleic acid. This molecule can interact with the surface trough one or two double bonds (L#1 and L#2 models, respectively). Figs. 2 and 3 show both types of interaction.

4. Kinetics of hydrogenation of monoene on Pd

The hydrogenation of monoenes involved the production of the saturated compounds and the *cis–trans* isomerization product among other reactions. The *cis–trans* isomerization was explained considering the formation of a half-hydrogenated surface intermediate and its easy rotation at the surface [24], whereas migration occurs via the π-allyl intermediate. Considering the oleic acid, the reactions that can occur are the formation of the *trans*-isomer elaidic acid (E) and the oleic hydrogenation to originate the saturated compound stearic acid (S). The adsorbed species can react reversibly

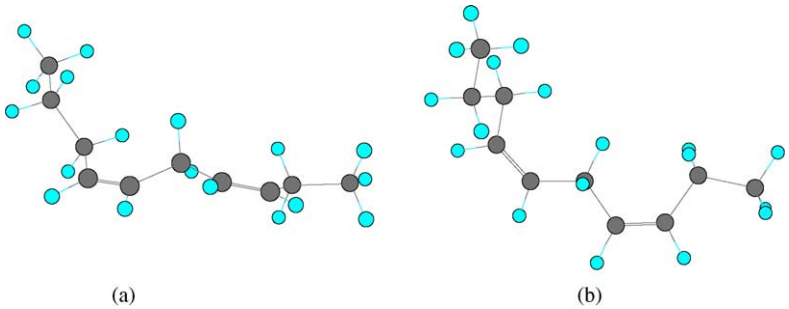

Fig. 3. L#2 model, side (a) and top view (b).

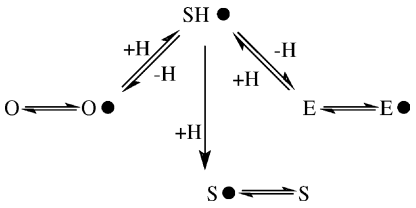

Scheme 1. Hydrogenation of oleic acid according to the Horiuti–Polanyi mechanism [24]: O, oleic acid; SH, half-hydrogenated; E, elaidic acid; i•, specie i adsorbed.

with a single hydrogen atom to form a half-hydrogenated SH• intermediate (see Scheme 1). The second hydrogen insertion is irreversible.

Considering additional possibilities, a pentacoordinated species was included in the calculation (denoted as SH_{PC}• in Scheme 2). Pentacoordinated species have been proposed in the case of several hydrogenation reactions, especially involving carbocations [25].

Monoene hydrogenation kinetics are often assumed to be first order in the concentration of unsaturated bonds [26], but orders varying between 0 and 1 have also been observed [27]. It is still a subject of debate whether *cis*/*trans* proceeds via the Horiuti–Polanyi mechanism with a σ-alkyl complex as a halfhydrogenated intermediate or via an abstraction-addition mechanism with a π-complex as intermediate. It is impossible to generalize the adsorbed monoyne mechanism because several experimental facts cannot be explained by this mechanism. Assuming a π-allyl intermediate for double bond migration, stability of the allylic intermediate from a *cis* or a *trans* will not be equal [30]. A *trans*-species would be more stable. Thus, in the case of double bond migration, the formation of the allyl complex is important to understand the experimental results.

Somorjai and co-workers [5] proposed that hydrogenation and isomerization reactions for *cis*-2-butene do not necessarily share the same alkyl intermediates. This mechanism is supported by the fact that *cis*-2-butene molecules decompose into 2-butyne on Pt surface [28]. This can also justify the absence of 1-butene in *cis*-2-butene isomerization. The other evidence is that the yields of *trans*-2-butene from *cis*-2-butene or 1-butene isomerization are different.

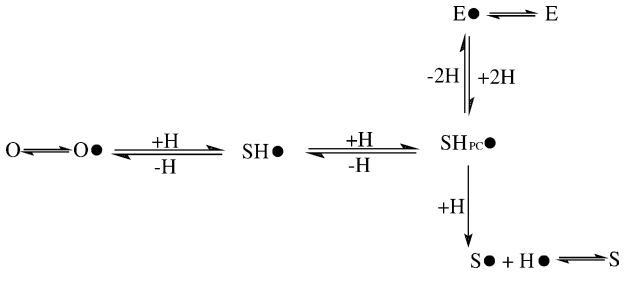

Scheme 2. Hydrogenation of oleic acid including a pentacoordinated species: O, oleic acid; SH, half-hydrogenated; E, elaidic acid; SH_{PC}, pentacoordinated species; i•, specie i adsorbed.

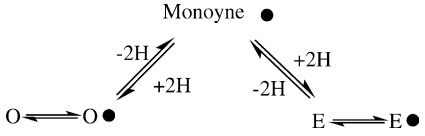

Scheme 3. Pathway for the hydrogenation of oleic acid including a monoyne species: O, oleic acid; SH, half-hydrogenated; E, elaidic acid; i•, specie i adsorbed.

Scheme 3 shows the pathway for the hydrogenation of oleic acid including a monoyne species. For any mechanism the double bond migration was not analyzed.

The main question to answer is which one of the three selected pathways for the reaction (*cis*/*trans* isomerization and/or hydrogenation) is more energetically favorable. According to Scheme 1 this would be:

1. A first potential reaction pathway concerns a half-hydrogenated species (in presence of hydrogen), which gives *trans*-monoene with the possibility of originating the saturated fatty acid (Scheme 1).
2. The second possible reaction pathway considers a pentacoordinated species with two H on the carbon coordinated with Pd, to give the *trans*-monoene or the saturated fatty acid (Scheme 2).
3. The third possible reaction mechanism involves an adsorbed monoyne (in presence or absence of hydrogen), to give *trans*-monoene (Scheme 3). In this case, the *trans*-monoene formation is related to the stability of the adsorbed monoyne on the surface. If the adsorbed monoyne were too much stable, no reaction of *cis*/*trans* isomerization would be observed. If the surface had Lewis acid-basic sites to abstract H^+ and H^- (close to a monoyne adsorbed on a Pd), the re-hydrogenation would be probably difficult. In this case, in order to give the *trans* species, the hydrogen must come from different sides of the adsorbed monoyne at the surface. For this situation to take place there must be enough hydrogen at the surface to overcome the tendency to render the same *cis* molecule.

The other main questions are: what is the surface ensemble size for this kind of reaction? And what is the desired surface structure for this kind of reaction? Considering the pathway involving the adsorbed monoyne, it would be necessary one Lewis acid (LA) site to adsorb the monoene, one acid–base pair (LA–LB at the Pd surface) to abstract a proton and an hydride and one acid–base pair as the supplier of H from the other side of the adsorbed monoene (that can be provided by H dissociated on Pd). If the adsorbed monoyne intermediates were excessively stable, the reaction would not continue. In particular, at low or null hydrogen pressures this deactivation would be possible.

Taking into account the properties of the supported palladium particles, there is no way to have oxidised palladium after previous reduction. There are Pd-H and Pd-H_2 species upon contact with hydrogen. The monoene is supposed to

be adsorbed on a Lewis acidic site. Pd Lewis acid and basic sites are necessary and the proportion would be 3LA:2LB or 1LA:1LB depending on the kind of mechanism selected. Being the accepted configuration of Pd $3d^{10}$ $4s^0$, it is clear that the surface Pd can receive hydrogen like proton or hydride. Upon adsorption is generally accepted that the surface Pd shift to a $3d^9 4s^1$ configuration [29].

The acidic properties of each Pd plane are related to the coordination number of the surface atoms. For supported Pd catalyst there are several forms of the metallic particle arrangement, among them, the octahedral or the cubooctahedral configuration. In all cases, variation in the size of the particle changes the proportion of exposed atoms. There are several potential changes in the electronic properties. The d band structure narrows as the particle size decreases. In this sense we must address the ensemble effect (steric effect) plus the filling of the d band (electronic effect) [11].

In view of all these published facts, our aim was to study: the Horiuti–Polanyi mechanism (Scheme 1), a new reaction pathway implicating a pentacoordinated species (Scheme 2) and a mechanism that originates an adsorbed monoyne (Scheme 3). It is extremely important to point out that no alkynes are detected in triglyceride hydrogenation. This species is proposed to remain at the surface, strongly adsorbed if hydrogen is absent or reacted to monoene (*cis* or *trans*) when hydrogen is present.

5. Results

5.1. Catalysts characterization

Table 2 lists the prepared catalysts and their metal content determined by atomic absorption spectroscopy (AAS) and Pd particle size determined from H_2 chemisorption.

Table 2 shows that catalysts prepared with $Pd(Acac)_2$ generated on the average smaller Pd particles than those the prepared with $Pd(NO_3)_2$ as it was predictable [35]. On the other hand, in the case of Pd(N)/ZSM5, it is evident that the Pd particles (diameter = 4.1 nm) are placed onto the zeolite external surface area. This is probably due to its particle size. The precursor $(NH_3)_4Pd(NO_3)_2$, was not able to get into the inner micropore area.

5.2. Catalytic activity test

5.2.1. Mass transfer effects

As mentioned before, the volumetric gas–liquid mass-transfer coefficient, $K_L a$, was separately measured at an excess of catalyst load [30]. The value obtained is in the 0.3–0.5 s^{-1} range and can be considered acceptable [4].

The Weisz–Prater criterion, Eq. (2), was used to evaluate the intraparticle diffusion limitations:

$$\Phi_I = \frac{(-r_{obs,i})\rho_p D_p^2}{D_{eff,i} C_i} \quad (2)$$

where $i = H_2$, TAG

A value of Φ_I smaller than 0.03–0.70 means that mass-transfer limitation for the unknown kinetics is negligible. The hydrogen concentration in the liquid was calculated following Andersson et al. [31]. Intraparticle diffusion coefficients for the catalysts were taken as $D_{H2} = 1.2 \times 10^{-8}$ m^2/s and $D_{TAG} = 1 \times 10^{-10}$ m^2/s [31]. The density of sunflower oil was determined from [32] as $\rho_{TAG} = 0.866$ g/ml, and tortuosity and porosity of catalyst (4 and 0.5, respectively) were obtained from [33]. In the present experiments, the numerical value of the Weisz–Prater modules of H_2 and TAG always remained above 0.7 indicating the existence of mass transference resistances.

The composition of the fatty acids at the end of the hydrogenation process is showed in Table 3. In all the cases, there was an increase in the concentration of stearic acid (C18:0) and a decrease in linoleic and linolenic acids (C18:2c and C18:3c) due to the saturation of the double bonds.

The iodine value (IV) of an oil or fatty acid is the weight of iodine with which it will combine, expressed as a percentage of its own weight. IV expresses the degree of unsaturation of the oil as:

$$IV = \frac{\text{grams of iodine absorbed}}{100 \text{ grams of oil}} \quad (3)$$

Simultaneously to the hydrogenation, two reactions take place: geometric isomerization (*cis–trans*) and positional isomerization (which we did not follow). Fig. 4 shows that formation of *trans*-isomers increases with the decreasing of IV, independently of the catalyst used. This result is somewhat

Table 2
Characterization of the catalysts: metallic load, particle size and BET surface area

Catalyst	Pd (wt.%)	d (nm)[a]	Precursor	Preparation	BET (m^{-2}/g)
Pd(A)/α-Al_2O_3	0.70	3.4	$Pd(Acac)_2$	WI[b]	9.5
Pd(A)/γ-Al_2O_3	0.78	1.8	$Pd(Acac)_2$	WI	137.0
Pd(N)/α-Al_2O_3	0.86	4.2	Pd $(NO_3)_2$	IWI[c]	9.5
Pd(N)/γ-Al_2O_3	0.77	3.9	Pd $(NO_3)_2$	IWI	137.0
Pd(N)/ZSM5	0.90	4.1	$(NH_3)_4Pd(NO_3)_2$	IWI	346.7

[a] Palladium particle size, d (nm) = 1.12/(Pd_e/Pd_t) [37], with Pd_e, exposed Pd and Pd_t, total Pd.
[b] WI: wet impregnation.
[c] IWI: incipient-wetness impregnation.

Table 3
Hydrogenation of sunflower oil: molar fraction (%)

Percentage	Sunflower oil	Oil partially hydrogenated				
		Pd (N)/γ-Al_2O_3	Pd(A)/γ-Al_2O_3	Pd(A)/α-Al_2O_3	Pd(N)/α-Al_2O_3	Pd(N)/ZSM5
C16:0	6.1	5.7	5.8	5.8	5.7	3.52
C18:0	3.4	7.9	17.5	7.6	6.9	8.25
C18:1t	0.0	28.4	43.7	23.6	18.7	24.46
C18:1c	35.2	48.8	30.0	49.8	50.2	58.85
C18:2t	1.4	4.6	0.8	5.3	3.4	2.52
C18:2c	52.6	3.3	0.9	6.5	13.7	1.99
C18:3c	0.4	0.1	0.0	0.1	0.1	0.00
C20:0	0.1	0.3	0.3	0.3	0.3	0.15
C22:0	0.1	0.7	0.7	0.7	0.7	0.23
trans	1.4	33.0	44.6	28.8	22.2	27.0
IV	124.9	80.2	66.4	83.9	89.4	79.45

Experimental condition: $T = 373$ K; $P = 413.5$ kPa; $t_{reaction} = 60$ min.

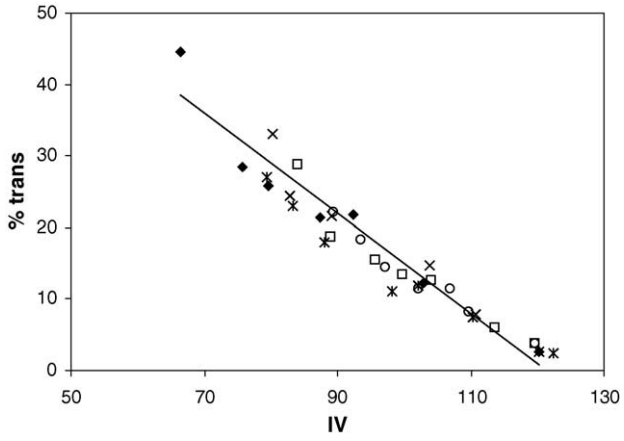

Fig. 4. Hydrogenation of sunflower oil. Iodine number (IV) vs. % of *trans*-isomer: (○) Pd (N)/α-Al_2O_3; (×) Pd (N)/γ-Al_2O_3; (♦) Pd(A)/γ-Al_2O_3; (□) Pd(A)/α-Al_2O_3; (*) Pd(N)/ZSM5.

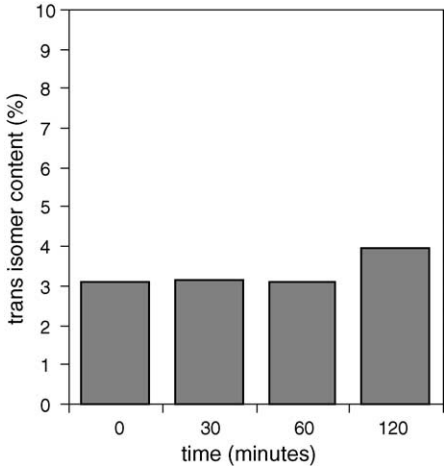

Fig. 5. The *trans*-isomer content at 453 K, without H_2.

disappointing. Our theoretical calculation will address this part in the next section.

In order to check the *cis–trans* isomerization without H_2, a different experiment was performed. Sunflower oil was heated up at 453 K in N_2 atmosphere, and then 0.5 g of a commercial Ni catalyst (Nysosel 222) was added. Samples were analyzed at different times. Fig. 5 shows that the *trans*-isomers production was insignificant, indicating that *cis–trans* isomerization takes place mainly in the presence of H_2.

5.3. Theoretical calculations for adsorption and reaction of oleic acid (cis-4-decene) on Pd(1 1 0), Pd(1 1 1) and Pd(0 0 1) planes

We studied the interaction of *cis*-4-decene with all the faces studied following a similar path:

- Adsorption of *cis*-4-decene in a π configuration (the C=C bond is parallel to the plane of the paper. Olefinic hydrogen atoms bond and the C=C bond are in a plane perpendicular to the surface (see Fig. 1B).

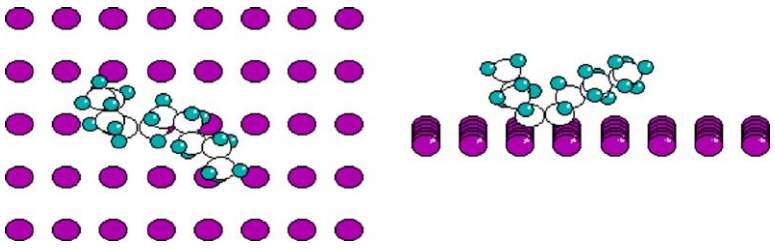

Fig. 6. *cis*-4-Decene with C_4 and C_5 hybridized at sp^3 over Pd(1 1 0). Top and side view.

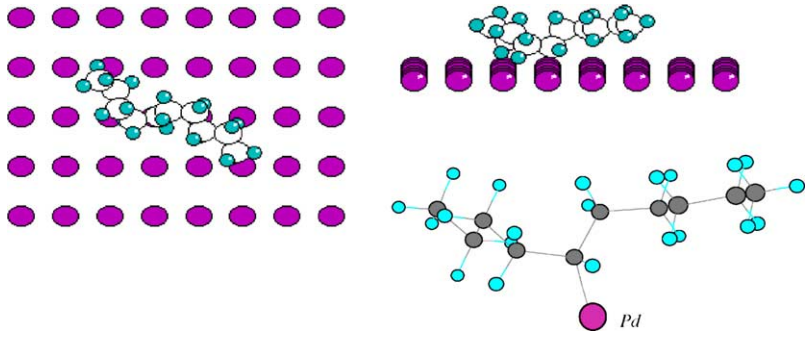

Fig. 7. Half-hydrogenated species on Pd(1 1 0). Top and side view.

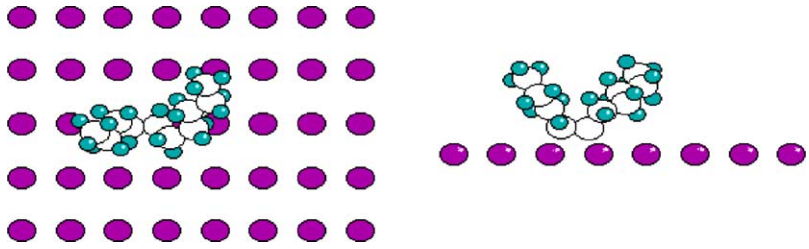

Fig. 8. *trans*-4-Decene on Pd(1 1 0). Top and side view.

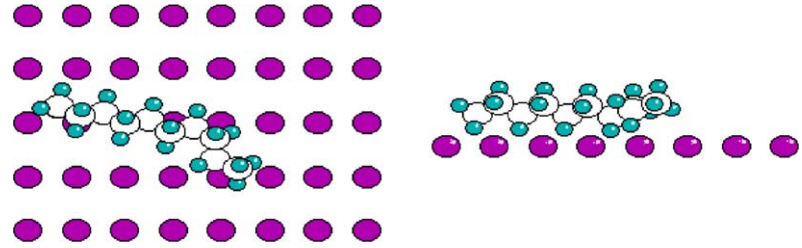

Fig. 9. Decane adsorption on Pd(1 1 0). Top and side view.

- Then, the adsorbed C atoms hybridize to near sp^3 state moving at di-σ position (Fig. 6).

Adsorption of *cis*-4-decene with the carbons of the double bond in sp^3 is conformationally less sterically hindered when it suffers at surface a transformation from *cis* to *trans* for the hydrogen atoms (25 kcal/mol versus 26 kcal/mol, respectively). This fact was checked with a model of the adsorbed decene on only two Pd atoms (using MM2).

Regarding the Horiuti–Polanyi mechanism, we studied the formation of the half-hydrogenated intermediate (see Fig. 7). Afterward, it was analyzed the subtraction of one H from the half-hydrogenated surface intermediate and the rotation at the surface, generating a *trans*-4-decene (Fig. 8). The adsorption

Table 4
Molecule-surface height (Å) and total and adsorption energies (eV) for the adsorption and reaction of *cis*-4-decene over Pd(1 1 1)

Species	Z (Å)[a]	E_{total} (eV)	$E_{adsorption}$ (eV)[d]	Comments
cis-4-Decene	2.6	−10225.7	−1.9	Ads- π $+2H_{ads}$
cis-4-Decene rehybridized sp^3	1.5	−10231.4		Ads-σ $+2H_{ads}$
H_2 adsorption	3.5	−9211.6	−0.4	
H_2 dissociation	1.2	−9213.3	−3.8	
Half-hydrogenated	3.5	−10224.3		$+1H_{ads}$ (ads. two-fold bridged site)
trans-4-Decene (ad)[b]	1.8	−10228.9		$+2H_{ads}$
trans-4-Decene[c]	2.7	−10227.3	−5.1	$+2H_{ads}$
Decane	3.0	−10222	−4.4	

[a] Z: molecule (C_4)-surface distance.
[b] *trans*-4-Decene (ad) has the decene with two C in sp^3 configuration.
[c] *trans*-4-Decene is the free molecule, with carbons from the double bond in sp^2.
[d] Adsorption energy for free molecules: $\Delta E_{ads} = \Delta E_{molecule/cluster} - \Delta E_{molecule} - \Delta E_{cluster}$.

Table 5
Molecule-surface height (Å) and total and adsorption energies (eV) for the adsorption and reaction of *cis*-4-decene over Pd(1 1 0)

Specie	Z (Å)[a]	E_{total} (eV)	$E_{adsorption}$ (eV)[d]	Comments
cis-4-Decene	2.7	−10037.8	−1.5	Ads-π + $2H_{ad}$
cis-4-Decene rehybridized sp^3	1.7	−10040.6		Ads-σ + $2H_{ad}$
H_2 adsorption	2.3	−9025.9	−0.4	
H_2 dissociation	1.4	−9029.0	−3.1	
Half-hydrogenated tetracoordinated	2.4	−10036.1		Ads-π + $1H_{ad}$
trans-4-Decene (ad)[b]	1.9	−10039.4		Ads-σ + $2H_{ad}$
trans-4-Decene[c]	2.4	−10040.0	−5.1	+$2H_{ad}$
Decane	3.1	−10035.4	−3.7	On top

[a] Z: molecule (C_4)-surface distance.
[b] *trans*-4-Decene (ad) has the decene with two C in sp^3 configuration.
[c] *trans*-4-Decene is the free molecule, with carbons from the double bond in sp^2.
[d] Adsorption energy for free molecules: $\Delta E_{ads} = \Delta E_{molecule/cluster} - \Delta E_{molecule} - \Delta E_{cluster}$.

Table 6
Molecule-surface height (Å) and total and adsorption energies (eV) for the adsorption and reaction of cis-4-decne over Pd(0 0 1)

Specie	Z (Å)[a]	E_{total} (eV)	$E_{adsorption}$ (eV)[d]	Comments
cis-4-Decene	2.4	−8008.1	−2.1	Ads-π + $2H_{ad}$
cis-4-Decene rehybridized sp^3	1.6	−8012.1		+$2H_{ad}$
H_2 adsorption	3.5	−6991.3	−0.1	
H_2 dissociation	1.3	−6995.8	−4.5	
Halfhydrogenated tetracoordinated	2.2	−8004.5		+$1H_{ad}$
trans-4-Decene (ad)[b]	1.5	−8005.4		+$2H_{ad}$
trans-4-Decene[c]	2.2	−8005.0	−5.6	+$2H_{ad}$
Decane	3.1	−8001.9	−4.6	

[a] Z: molecule (C_4)-surface distance.
[b] *trans*-4-Decene (ad) has the decene with two C in sp^3 configuration.
[c] *trans*-4-Decene is the free molecule, with carbons from the double bond in sp^2.
[d] Adsorption energy for free molecules: $\Delta E_{ads} = \Delta E_{molecule/cluster} - \Delta E_{molecule} - \Delta E_{cluster}$.

of the products (decane, in Fig. 9 and *trans*-4-decene) and the adsorption and dissociation of H_2 were also considered.

Tables 4–6 present the results for the three main Pd planes. The energies are presented as absolute energies, because it is impossible find normalization. This work is focused in the mechanism and how the atoms are reordering during this mechanism.

Table 4 presents adsorption energy, molecule-surface separation and total energy for the species above mentioned on Pd(1 1 1). Similar qualitative results were observed for Pd(1 1 0) and Pd(0 0 1) as shown in Tables 5 and 6, however, higher adsorption energy was found for the Pd(0 0 1) face.

Considering the reaction pathway implicating a pentacoordinated species (Fig. 10), the hydrogen addition is not energetically favored with respect to the halfhydrogenated species. The system Pd(0 0 1) + *pentacoordinated* species + H_{ad} presented a total energy of −8001.8 eV.

Regarding the mechanism that originates an adsorbed monoyne, Table 7 shows the total energy for this species on the three planes studied.

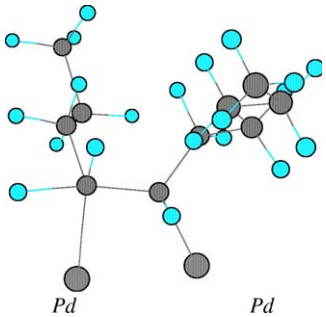

Fig. 10. Pentacoordinated species.

5.4. Adsorption of cis-4,cis-7-decediene on Pd(1 1 1), Pd(1 1 0) and Pd(0 0 1)

The interaction of *cis*-4,*cis*-7-decediene with the surface takes place through one (L#1 model, Fig. 2) or both double bonds (L#2 model, Fig. 3). Table 8 shows the adsorption energy and total energy of these models over the three planes analyzed. L#1 model was favored in all the Pd faces. Even more, the highest adsorption energy was found for Pd(0 0 1).

Table 7
Molecule-surface separation (Å) and total energy (eV) for the monoyne species over Pd(0 0 1), Pd(1 1 1) and Pd(1 1 0) (plus $4H_{ad}$ in order to compare with halfhydrogenated species)

Plane	Z (Å)[a]	E_{total} (eV)
Pd(0 0 1)	1.7	−8012.2
Pd(1 1 1)	1.5	−10238.5
Pd(1 1 0)	0.8	−10048.3

[a] Z: molecule (C_4)-surface distance.

Table 8
Molecule-surface separation (Å) and adsorption energy (eV) for *cis*-4,*cis*-7-decediene over Pd(0 0 1), Pd(1 1 1) and Pd(1 1 0)

Pd face	Specie	*Z* (Å)[a]	*E* (eV)	Comments
(0 0 1)	L#1	2.6	−5.3	Ads-σ
(0 0 1)	L#2	2.1	−3.9	Ads-σ
(1 1 1)	L#1	2.6	−4.9	Ads-σ
(1 1 1)	L#2	2.2	−3.3	Ads-σ
(1 1 0)	L#1	2.4	−4.0	–
(1 1 0)	L#2	2.3	−2.4	–

[a] *Z*: molecule (C_4)-surface distance.

However, the existence of L#2 model is also possible over all the planes.

6. Discussion

Experimental results showed that it was not possible to modify *cis*/*trans* selectivity changing Pd particle size using different material support. Pd catalysts prepared with $Pd(Acac)_2$ or $Pd(NO_3)_2$ precursors originate different particle size [13,34], and this difference is remarkable when the supports present different specific surface area. This is the case of Pd(A)/γ-Al_2O_3 and Pd(N)/α-Al_2O_3 with particle diameters of 1.8 and 4.2 nm, respectively. However, these catalysts presented the same *cis*/*trans* selectivity.

The effect of pore size distribution in the *cis*/*trans* selectivity cannot be discussed here because the Pd particles were placed in the zeolite external surface area. Thus, we have to look for a different explanation for the *cis*/*trans* selectivity during the hydrogenation of sunflower oil. It is important to remark that the reaction is a three-phase process that in our case presents intraparticle transport limitations as it was shown through the calculus of the Weisz–Prater modulus. It means that there is very low H_2 concentration on the catalysts's surface. Regarding the triglyceride molecule, the intraparticle diffusion of oil molecules can be neglected, because their concentrations are always much greater than the hydrogen concentration [4]. On the other hand, others authors indicated that the high trygliceride Weisz–Prater value pointed out the difficulty in the mobility of the bulky molecule. In this concept we based the catalysts model, which consider a not H_2 saturated catalyst surface

Although EHMO is approximated, our results are of enough quality to use them as an additional tool of characterization. Furthermore, results from higher level calculations [11] mention that the metal-C bond has a length of 1.98 Å (Pd-C_2H_4), whereas Pd-H involves 1.54 Å. Our results for Pd-C bond length are 1.5, 2.4 and 2.22 Å for the (1 1 1) (1 1 0) and (1 00) planes, respectively. On the other hand the metal–H bond length are 1.2, 1.4 and 1.3 Å for the same planes. In the same line, Fahmi and van Santen [35] determined a 39 kcal/mol the adsorption of ethylene on Pd. Our results for *cis*-decene adsorption are in the 35–50.2 Kcal/mol range for the different Pd planes studied.

In the case of Pd(1 1 1) the model compound *cis*-4-decene is π-adsorbed (−1.91 eV) and then hybridizes to near sp^3 state moving to a di-σ position (−5.7 eV). Concerning the adsorption and dissociation of H_2, as it was expected, they were energetically favorable (−0.41 and −3.79 eV, respectively). We found an activation energy for the formation of the half-hydrogenated intermediate, with a change in the total energy of +7.1 eV. Afterwards, the subtraction of one H was analyzed from the half-hydrogenated surface intermediate and the rotation at the surface, generating an adsorbed *trans*-4-decene. This step was energetically favored (−4.1 eV) comparing with the hydrogenation from the same intermediate (+2.3 eV). On the subject of products adsorption, it was observed that the sequence of desorption is as follow: decane > *cis*-4-decene (−3.7 eV) > *trans*-4-decene (−6.9 eV) all energies refereed to decane. In comparison, adsorption of *trans* decene is preferred. It can be concluded that once the second H is added, the decane is easily desorbed.

In the case of Pd(1 1 0) the model compound *cis*-4-decene is π-adsorbed (−1.47 eV) and then hybridizes to near sp^3 state moving to a di-σ sigma position, again (−2.71 eV). Concerning the adsorption and dissociation of H_2, they were energetically favorable (−0.39 and −3.07 eV, respectively). We found an activation energy for the formation of the half-hydrogenated intermediate, with a change in the total energy, of +4.5 eV. The subtraction of one H was analyzed from the half-hydrogenated surface intermediate and the rotation at the surface, generating a *trans*-4-decene adsorbed. This step was energetically favored (−0.6 eV) comparing with the hydrogenation from the same intermediate (+0.7 eV). Regarding the products adsorption, it was observed that the sequence of desorption is as follow: decane > *cis*-4-decene (−2.4 eV)> *trans*-4-decene(−4.6 eV) all energies refereed to decane.

In the case of Pd(1 0 0), the model compound *cis*-4-decene is also π-adsorbed (−2.10 eV) and then the next step presents a similar energy than on Pd(1 1 0) (−1.9 eV). The generation of *trans*-decene adsorbed step was energetically favored (−0.4 V) comparing with the hydrogenation from the same intermediate. Considering the products, it was observed that the sequence of desorption is as follows: decane (−8001.9 eV) *cis*-4-decene (−8002. 95 eV) *trans*-4-decene (−8005.4 eV).

The half-hydrogenated intermediate formation is the rate-determining step in the Horiuti–Polanyi mechanism. The reaction of full hydrogenation is considered to be exothermic in −0.9 to −1.15 eV, whereas (as well as) the *cis*/*trans* isomerization is exothermic in −2 eV (0 0 1), −5.5 eV (1 1 0) and −3.2 eV (1 1 1). The formation of the adsorbed monoyne completes the picture. Experimentally we found that no elaidic acid is obtained without hydrogen present. We need hydrogen to hydrogenate a very stable surface species. The formation of the monoyne adsorbed in the three planes showed a difference in energy comparing with the intermediary half hydrogenated of −7.7 eV for Pd(0 0 1), −14.4 eV for Pd(1 1 1) and −12.2 eV for Pd(1 1 0). Metal–carbon distances ranged in this case from 0.8 to 1.7 A (see Table 7).

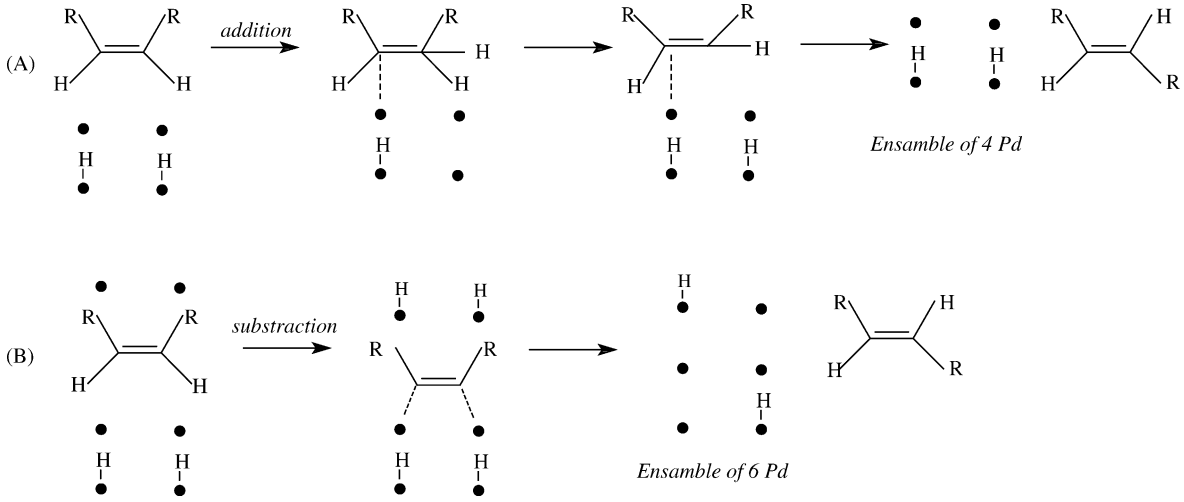

Scheme 4. Proposal for the formation of the *trans*-isomer from the half-hydrogenated intermediate (A) or from the adsorbed monoyne (B): (●) Pd.

These values are an indication of the strong adsorption of the monoyne at the three Pd planes and explain why there is not *cis–trans* isomerization without hydrogen. If hydrogen is present, hydrogenation takes place.

The main result of the combination of the experimental and theoretical results is that the preferred pathway involves always the formation of two different intermediates in the case of a model of reaction of *cis*-monoene. Both intermediate can produce the *trans*-isomer and only the half hydrogenated will produce the fully hydrogenated fatty acid. The main route for *trans*-monoene formation seems to be, from the thermodynamic point of view, the monoyne pathway being secondary the Horiuti–Polanyi mechanism, at least on the studied models of Pd planes.

In the case of the adsorbed monoyne, the intermediate is very stable to be hydrogenated with the hydrogen resulting from the dehydrogenation itself. It needs labile hydrogen. Even more, the dehydrogenation step is too much exothermic to generate the *cis*-isomer. The *trans*-isomer is more near in energy to this intermediate than the *cis* one.

Whatever the plane considered, the half intermediate is the rate-limiting step. Moreover, the intermediate thermodynamics can be affected by the plane structure, but the 4-*trans*-decene formation is favoured instead the *cis*-isomer or the fully hydrogenated compound. Scheme 4 shows the proposal for the formation of the *trans*-isomer from the half-hydrogenated intermediate or from the adsorbed monoyne.

For these mechanisms, geometric requirements are different: we need 4 or 6 Pd atoms at surface, necessarily close for Horiuti–Polanyi and monoyne mediated mechanism, respectively. The *trans*-monoene formation implies the reaction of hydrogen atoms adsorbed with the monoyne adsorbed in the middle of them. There are geometric conditions to the *cis*-isomers formation. The oleic acid suffers from H-abstraction or H-addition on Pd surface. The resulting species, being the half-hydrogenated or the adsorbed monoyne, have the possibility to add hydrogen from the same side (*cis*) or from different sides (*trans*). The addition from the same side, in the case of the adsorbed monoyne, is the reversal of the adsorbed monoyne formation that is very exothermic. The resulting species must be at least more stable than the original one and this is the case of the *trans*-monoene. To produce the *trans*-monoene hydrogen, it is necessary H from different H_2 molecules or from monoene H-abstraction (see Scheme 4). Another alternative is that the change from *cis* to *trans*-isomer takes place during the adsorption of the monoene itself. The change is not thermodynamically favored (+2.5 eV for Pd(1 1 1), +1.2 eV for Pd(1 1 0), +2.7 eV for Pd(0 0 1)). Experimental data also allows us to conclude that it is not the main route of *trans*-isomers formation.

The transition from the 4-*cis*-decene adsorbed with two C like sp^3 to the half-hydrogenated species implies a change in conformation. From the half-hydrogenated, H atom is lost and placed near the surface (shown by the arrow in Fig. 11). Then, when the H is lost the *trans*-monoene structure is the most probable: +26.7 kcal/mol for *cis*-isomer and +25.3 for *trans*-isomer. The distances of the species to the surface (although close to bond length) are long enough to make the reactions structure insensitive for the three Pd planes evaluated. The bond between the Pd atoms and the carbon atoms is long enough to make the effect of the neighbor less important that the strength of the bond itself, at least in these three planes. If the plane introduces steric restrictions through the presence of kinks/steps, terraces or defects, is probable that the results will change if the adsorption takes place on those defects. An alternative way to modify the selectivity can be the use of an additive to introduce steric and electronic effects [36].

The coordination of *cis*-4,7-decadiene is possible through one or both double bonds. Both species are energetically stable. The model of linoleic acid is adsorbed in the di σ form, but maintaining the bond length of double bond. This

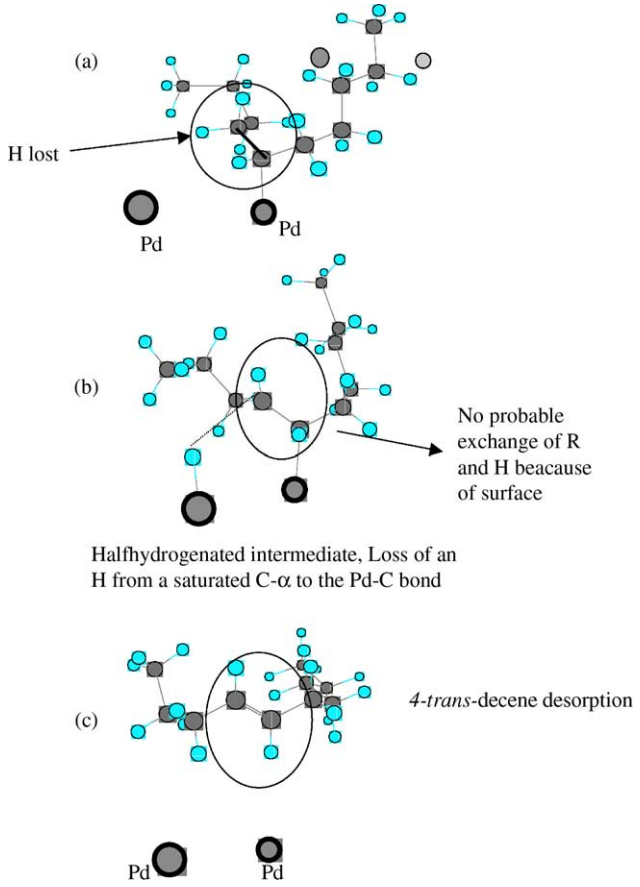

Fig. 11. Formation of *trans*-monoene from the half-hydrogenated intermediary: Pd atom (●); C atom (●); H atom (●); R, alkyl chain.

theoretical result is in agreement with the results obtained for 1,3-butadiene on Pd published by Delbecq and co-workers [12]. Diene molecules without distortion are adsorbed in the di-σ form without important changes in its structure on Pd planes. Addition would be probably easier than subtraction. Future works will deal with the mechanism of formation of the *cis*/*trans* monoene from the diene and the double bond migration through the allyl-intermediate formation by abstraction of hydrogen of a saturated carbon α to a double bond.

7. Conclusions

No sensibility to the structure was found in sunflower oil hydrogenation on supported Pd. For all of the supports and particle size used in this study, a linear relationship between iodine value and *trans*-isomers formation was determined. Thus, there is no simple way to control selectivity through the support selection or the particle size distribution at least for Pd under described preparation procedures.

The EHMO studies show that both mechanisms (Horiuti–Polanyi and monoyne-mediated) are possible for *trans*-monoene formation on the Pd planes, but the monoyne-mediated mechanism is always energetically more exothermic. A mechanism through a pentacoordinated species can be ruled out. The formation of *trans*-monoene isomers is conditioned by the mechanism itself, not by the metal/support interaction. The approach of combining MM2 plus EHMO demonstrated to give useful results that can be related to the experimental work.

Acknowledgements

Authors thank the Universidad Nacional del Sur (UNS) and the Consejo Nacional de Investigaciones Científicas y Técnicas (CONICET) for their financial support.

References

[1] R. Mensink, M. Katan, N. Engl. J. Med. 323 (1990) 439.
[2] A. Ascherio, M. Katan, P. Zock, M. Stampfer, W. Willett, N. Engl. J. Med. 340 (1999) 1994.
[3] D. Jovanovic, R. Radovic, L. Mares, M. Stankovic, B. Markovic, Catal. Today 43 (1998) 21.
[4] E. Santacesaria, P. Parrella, M. Di Sergio, G. Borrelli, Appl. Catal. A 116 (1994) 269.
[5] C. Yoon, M. Yang, G. Somorjai, J. Catal. 176 (1998) 35.
[6] A. Teplyakov, B. Bent, J. Am. Chem. Soc. 117 (1995) 10076.
[7] K. Kikataura, S. Obaras, K. Morokuma, J. Am. Chem. Soc. 103 (1981) 2891.
[8] J. Noell, P. Hay, J. Am. Chem. Soc. 104 (1982) 4578.
[9] S. Obaras, K. Kikataura, K. Morokuma, J. Am. Chem. Soc. 106 (1984) 7482.
[10] J. Low, W. Goddard, J. Am. Chem. Soc. 106 (1984) 8321.
[11] A. Dedieu, Chem. Rev. 100 (2000) 543, and references therein.
[12] A. Valcárcel, A. Clotet, J. Ricart, F. Delbecq, P. Sautet, Surf. Sci. 549 (2004) 121.
[13] L. Konopny, A. Juan, D. Damiani, Appl. Catal. B 15 (1998) 115.
[14] O. Stenberg, N.-H. Schöön, Chem. Eng. Sci. 40 (1985) 2311.
[15] P. Weisz, D. Prater, Adv. Catal. 6 (1954) 143.
[16] R. Hoffmann, J. Chem. Phys. 39 (6) (1963) 1397.
[17] R. Sumerville, R. Hoffmann, J. Am. Chem. Soc. 98 (1976) 23.
[18] P. Hay, J. Thibeault, R. Hoffmann, J. Am. Chem. Soc. 97 (1975) 4884.
[19] I. Chamber, L. Forrs, G. Calzaferri, J. Phys. Chem. 93 (1989) 5366.
[20] A. Anderson, R. Hoffmann, J. Chem. Phys. 60 (1974) 4271.
[21] W. Lotz, J. Opt. Soc. Am. 60 (1970) 206.
[22] A. Vela, J. Gázquez, J. Phys. Chem. 92 (1985) 5366.
[23] A. Rochefort, J. Andzelm, N. Russo, D. Salahub, J. Am. Chem. Soc. 112 (1990) 8239.
[24] J. Horiuti, M. Polanyi, Trans. Faraday Soc. 30 (1934) 1164.
[25] B. Gates, J. Katzer, G. Schuit, Chemistry of Catalytic Process, McGraw Hill, New York, 1975.
[26] G. Colen, G. Van Duijn, H. Van Oosten, Appl. Catal. 43 (1988) 339.
[27] J. Lindelfelt, J. Magnusson, N.-H. Schöön, J. Am. Oil Chem. Soc. 60 (1983) 603.
[28] M.A. Chesters, C. de la Cruz, P. Gardner, E.M. McCash, P. Pudney, G. Shahid, N. Sheppard, J. Chem. Soc., Faraday Trans. 86 (1990) 2757.
[29] C. Moore, Atomic Energy Levels as Derived from the Analyses of Optical Spectra, U.S. Goberment Printing Office, Washington, DC, 1971.

[30] O. Stenberg, N.-H. Schöön, Chem. Eng. Sci. 40 (1985) 2311.
[31] K. Andersson, M. Hell, L. Löwendahl, N.-H. Schöön, J. Am. Oil Chem. Soc. 51 (1974) 171.
[32] R. Allen, M. Formo, R. Krishnamurthy, G. McDermott, F. Norris, N. Sonntag, in: D. Swern (Ed.), Baileyĭs Industrial Oil and Fat Products, vol. 2, fourth ed., John Wiley & Sons Publication, 1982.
[33] H. Fogler, Elements of Chemical Reaction Engineering, second ed., Prentice Hall International Editions, 1992.
[34] G. Tonetto, D. Damiani, Int. J. Chem. React. Eng. 2 (2004) A10.
[35] A. Fahmi, R. van Santen, J. Phys. Chem. 100 (1996) 5676.
[36] B. Nohair, C. Especel, G. Lafaye, P. Marecot, L. Hoangb, J. Barbier, J. Mol. Catal. A 229 (2005) 117.
[37] P.C. Aben, J. Catal. 10 (1968) 224.